Short communication

A stable $La_{1.95}Ca_{0.05}Ce_2O_{7−\delta}$ as the electrolyte for intermediate-temperature solid oxide fuel cells

Zetian Tao, Lei Bi, Shuming Fang, Wei Liu*

CAS Key Laboratory of Materials for Energy Conversion, Department of Materials Science and Engineering, University of Science and Technology of China, 96 Jinzhai Road, Hefei, Anhui 230026, People's Republic of China

ARTICLE INFO

ABSTRACT

The $La_{1.95}Ca_{0.05}Ce_2O_{7−\delta}$ (LCCO) material is successfully synthesized using the Pechini method. The synthesized powders are exposed to atmospheric CO_2 and H_2 with 3% H_2O at 700 °C. The treated LCCO powders are investigated using X-ray diffraction (XRD) to study the chemical stability. According to the XRD results, LCCO is very stable and shows no reactions with CO_2 or H_2O. A fuel cell with the LCCO electrolyte is prepared using the suspension spray method and is tested in the range from 600 °C to 700 °C using humidified hydrogen (∼3% H_2O) as the fuel and static air as the oxidant. An open-circuit potential of 0.832 V and a maximum power density of 259 mW cm$^{−2}$ are obtained for a single cell with an interface resistance of 0.23 Ω cm^2 at 700 °C.

© 2011 Elsevier B.V. All rights reserved.

1. Introduction

Solid oxide fuel cells (SOFCs) have attracted increasing attention worldwide because of the demand for clean, secure, renewable energy [1,2]. The oxide-ion-conducting SOFCs, which require high operating temperatures to lower ohmic losses, have been the most widely used. However, the operating costs of these SOFCs systems have been too expensive when the fuel cells were operated at high temperatures. A reduction in the SOFC working temperature is urgently required for broad commercialization [3,4]. Doped CeO_2 and proton-conducting SOFCs have been used to satisfy this demand [5–7]. In particular, the proton-conducting SOFCs have attracted more attention due to its low activation energy [8] and high energy efficiency [9].

Many ABO_3-type perovskites, particularly the rare earth doped $BaCeO_3$ materials, which exhibit higher proton conductivities, have been used as the electrolyte for the proton-conducting SOFCs [10–14]. However, high proton conductivity and stability seem to be antagonistic, as investigated by Kreuer [15] and Norby and Larring [16]. Several studies to improve the stability of $BaCeO_3$ have been conducted by our group [17,18]. Furthermore, doped $BaZrO_3$ materials have also been used as the electrolyte because of their high chemical stability [19]. However, $BaCeO_3$ are still too unstable to fulfill the needs of commercial application and $BaZrO_3$ also displays problems with high sintering temperatures

and low proton conductivity [20]. Other structural materials have also been used as the electrolyte for proton-conducting SOFCs, such as $LaNbO_4$ for its high stability [21]. The Ca^{2+} doped disordered fluorite structure (found in $La_2Ce_2O_7$, space group Fm3m) has been investigated for its proton conductivity and is used for the ammonia formation [22,23]. Recently, we proved the proton conductivity using a hydrogen permeation experiment [24]. The disordered fluorite structure could also be used as the electrolyte for the SOFCs.

In this study, the chemical stability of the $La_{1.95}Ca_{0.05}Ce_2O_{7−\delta}$ (LCCO) powders was studied under atmospheric CO_2 and H_2O, and no reactions were found during the experiment. Then, the LCCO was used as the proton-conducting electrolyte using a suspension spray method combined with an in situ sintering method [25] to assemble a single fuel cell. Electrochemical properties of the fuel cell were also studied.

2. Experimental

LCCO powders were synthesized using the Pechini method. First, a nitrate solution was prepared by dissolving the appropriate stoichiometric ratios of $Ce(NO_3)_3·6H_2O$ in a beaker. Then, the La_2O_3 and $CaCO_3$ in the appropriate stoichiometric ratio were dissolved in nitric acid and mixed with the prepared solution of $Ce(NO_3)_3$. The appropriate amount of citrate acid was then added. The solution was heated under stirring to evaporate water until it changed into a viscous gel and finally ignited in a flame, resulting in white ash. The ash was calcined at 500 °C for 3 h to form fine LCCO powders. The powders were treated under 3% CO_2 and 3% H_2O at 700 °C

* Corresponding author. Tel.: +86 551 3606929; fax: +86 551 3601592.
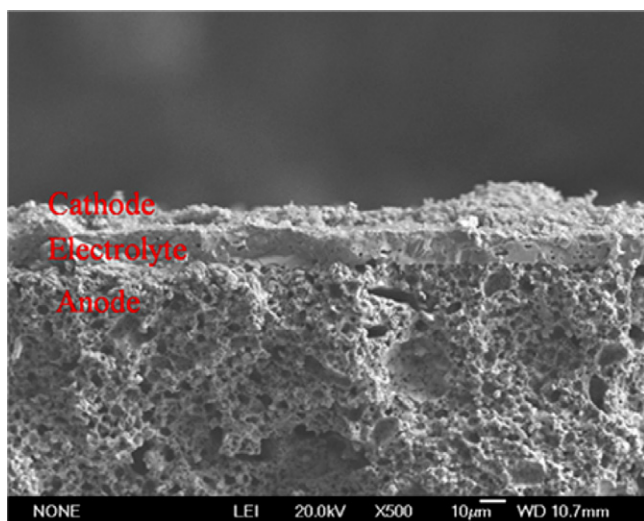E-mail address: wliu@ustc.edu.cn (W. Liu).

Fig. 1. X-ray diffraction patterns of $La_{1.95}Ca_{0.05}Ce_2O_{7-\delta}$ powders after exposure to the 3% CO_2 and 3% H_2 atmosphere with 3%H_2O at 700 °C for 100 h.
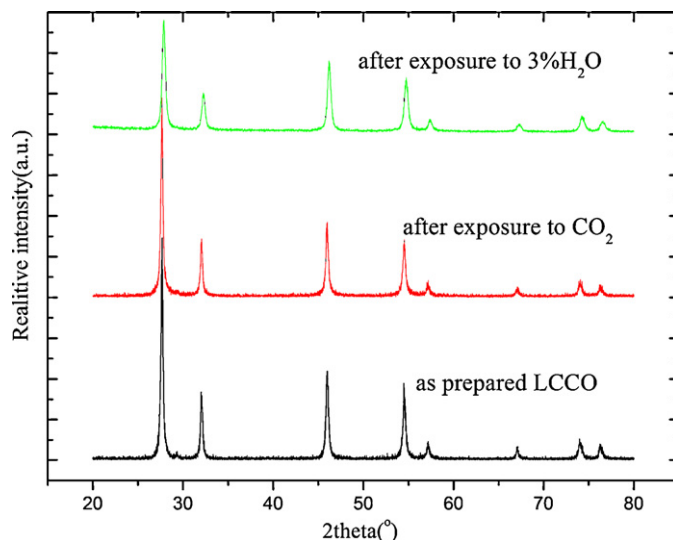

Fig. 2. Cross-section views of the cell assembled with the electrolyte of LCCO without surface modification.

for 100 h. The change of the phase was examined with an X-ray diffractometer (XRD) using CuKα radiation.

These pre-LCCO powders were mixed well with NiO in a weight ratio of 40:60. To produce sufficient porosity in the anode, 20 wt.% starches was added as the pore former. The mixed powders were placed under 250 MPa of pressure with 15 mm in diameter and 0.5 mm in thickness and subsequently fired at 700 °C for 3 h as anode substrates. The LCCO membrane was fabricated on the anode substrate using an in situ reaction. The LCCO powders were dispersed into ethanol by ball-milling for 24 h to form a suspension. The suitable organic additives (triethanolamine, benzyl butyl phthalate and polyvinyl butyral) were added into the suspension, which was employed to distribute the metal oxides and the carbonate in the ethanol. The solid ratio of the starting materials was 5 wt.%. The suspension was directly deposited on the anode substrate. Then, the bi-layers of green electrolyte and anode were co-fired at 1450 °C in air for 5 h. A mixture of $LaSr_3Co_{1.5}Fe_{1.5}O_{10-\delta}$ (LSCF) [26] and LCCO was printed on the electrolyte of the half-cell and then fired at 1000 °C for 3 h to form a porous cathode.

The electrode active area was 0.237 cm². Ag paste was applied to the electrode as a current collector. Electrochemical measurements of the fuel cell were performed in an Al_2O_3 test housing that was placed inside a furnace. Humidified hydrogen (~3% H_2O) was fed into the anode chamber at a flow rate of 25 mL min⁻¹, while the cathode was exposed to atmospheric air. The anode side was sealed with Ag paste. Fuel cell performance, based on the *I–V* curves was measured with a DC Electronic Load (IT8511). Impedance of the cell under open circuit conditions was measured using a CHI604B electrochemical instrument (0.1 Hz to 100 kHz). A scanning electron microscope (SEM, JSM-6301F) was employed to observe the fracture morphology of the assembled cell.

3. Results and discussion

As shown in Fig. 1, the LCCO powders show a fluorite structure without the formation of other phases. To investigate the chemical stability, the powders are exposed to 3% CO_2 and 3% H_2O at 700 °C for 100 h. The XRD patterns, shown in Fig. 1, after exposure to these
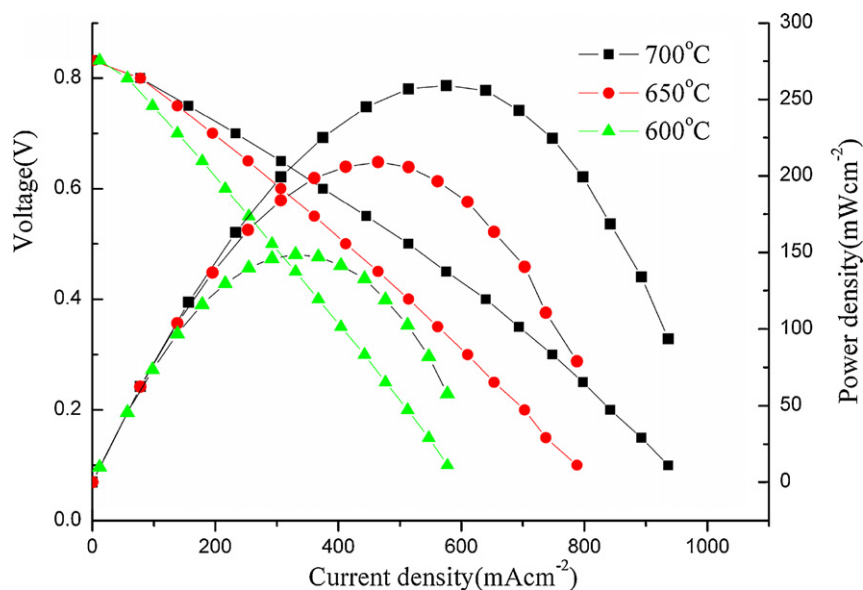

Fig. 3. Performance of a single cell under a wet hydrogen atmosphere at different temperatures.
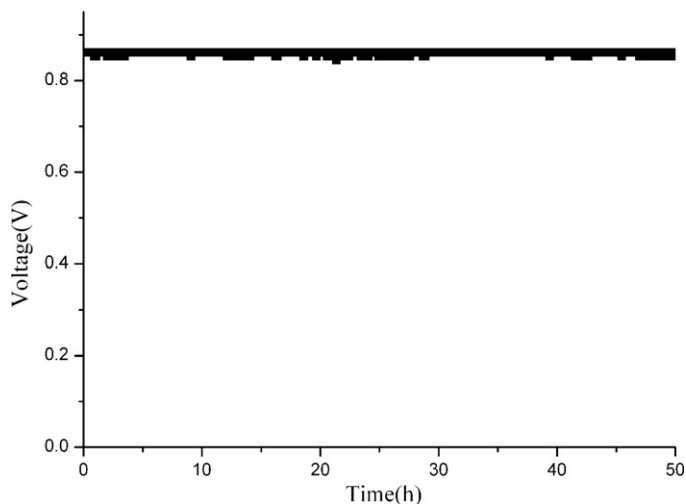
Fig. 4. Long-term performance of the cell at 600 °C under work conditions.
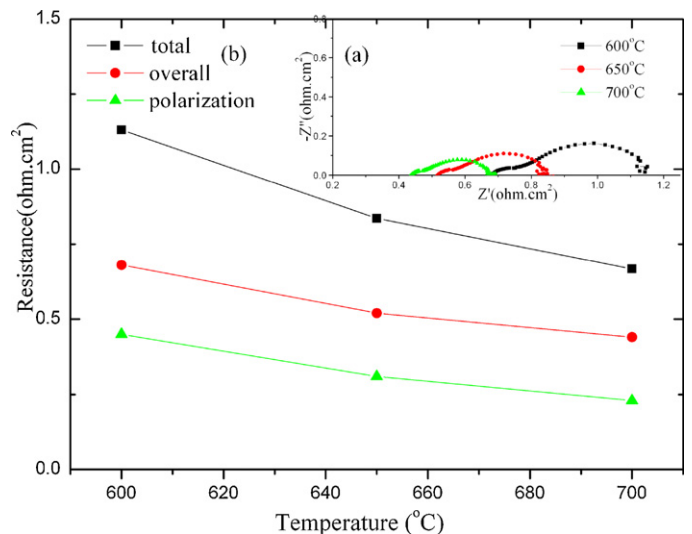

Fig. 5. (a) Impedance spectra and (b) the interfacial polarization resistances, electrolyte resistances, and total resistances determined from the impedance spectra of the as-prepared cell measured under open-circuit conditions at different temperatures.

conditions remain unchanged, demonstrating that the LCCO powders are stable in an atmosphere containing 3% CO_2 and 3% H_2O. We know that the rare earth doped $BaCeO_3$ materials, which can easily react with CO_2 and H_2O is the traditional proton-conducting electrolyte [14].

$$BaCeO_3 + CO_2 \rightarrow 0.8CeO_2 + BaCO_3 \qquad (1)$$

$$BaCeO_3 + H_2O \rightarrow 0.8CeO_2 + Ba(OH)_2 \qquad (2)$$
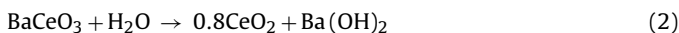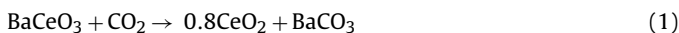
The reactions of the electrolyte materials above can destroy the cell system and reduce the OCV of the assembled cell due to gas leaks. The fluorite structure LCCO does not react with 3% H_2O and CO_2 at 700 °C for 100 h, which indicates that this material is more stable than many other electrolyte materials. Because of its high chemical stability, LCCO can be used as an electrolyte for SOFCs.

Fig. 2 shows the cross-sectional view of the single cell which is sintered at 1450 °C in air for 5 h. As shown, the LCCO electrolyte is approximately 15 μm in thickness and adhered well to the anode and cathode. The fine structure can lower the interfacial polarization resistance to improve the fuel cell performance. From the figure, we also know that the electrolyte is dense which can assure a high open-circuit potential.

Fig. 3 presents the I–V and I–P characteristics of the as-prepared cell measured from 600 to 700 °C with humidified hydrogen (∼3% H_2O) as the fuel. The maximum power densities of 259, 209, and 149 mW cm^{-2} with the OCV values of 0.832, 0.847 and 0.861 V, respectively, are obtained at 700, 650 and 600 °C, respectively. The OCV of this material is lower than that of the traditional proton-conducting electrolyte at various temperatures; the reduction of Ce^{4+} to Ce^{3+} provided the electronic conductivity, which lowers the OCV. Although the OCV is lower compared to the traditional proton-conducting electrolyte, the performance of the cell can be compared with the $BaCeO_3$-based fuel cell [27]. The single cell is kept stable in the testing condition of 600 °C, as shown in Fig. 4. From Fig. 4, we can see that the OCV of the cell is kept almost constant under the working conditions which further prove the chemical stability of LCCO. The resistance of the cell under open circuit conditions, which was investigated by AC impedance spectroscopy, is shown in Fig. 5(a). The high frequency intercept corresponds to the overall electrolyte resistance of the cell including ionic resistance of the electrolyte and some contact resistance associated with the interfaces [28]. The low frequency intercept corresponds to the total resistance of the cell. Therefore, the difference between the high frequency and low frequency intercepts with the real axis represents the total interfacial polarization resistance (R_p) of the

cell. As shown in Fig. 5(b), the total resistance of the cell significantly decreases with the increase in temperature, typically from 1.13 Ω cm^2 at 600 °C to 0.67 Ω cm^2 at 700 °C. The low resistance is comparable to other proton-conducting electrolytes, but the cell performance is lower because of the low open-circuit potential. The open-circuit potential can be increased by adding an additional layer such as ScSZ or YSZ [29,30]. Then the novel electrolyte can be used as a potential electrolyte for the SOFCs by increasing the low open-circuit potential.

4. Conclusion

LCCO powders were synthesized by the Pechini method and the XRD patterns indicated that this material had a fluorite structure. The powders were exposed to 3% CO_2 and 3% H_2O at 700 °C for 100 h to determine the chemical stability, which is urgently required for commercial applications of SOFCs. The unchanged XRD peaks validated the chemical stability of the LCCO and made it a potential electrolyte material for use in SOFCs. With a mixture of LSCF and LCCO as the cathode and a wet suspension approach, a single cell with LCCO as the electrolyte was assembled and tested. The maximum power density of the single cell was 259 mW cm^{-2} at 700 °C. The overall resistance was 0.44 Ω cm^2 and the polarization resistance of the electrode was 0.23 Ω cm^2 at 700 °C. At 700 °C, the open-circuit potential was only 0.832 V because the electronic conductivity was produced when Ce^{4+} was reduced to Ce^{3+}. Although the cell performance was lower than that of the traditional proton-conducting SOFCs, the high chemical stability and the possibility of increasing the open-circuit potential with a bi-layer electrolyte indicate that the material can a potentially be a commercially useful electrolyte in SOFCs.

References

[1] Z.P. Shao, S.M. Haile, Nature 431 (2004) 170.
[2] T. Norby, Solid State Ionics 125 (1999) 1.

[3] B.C.H. Steele, A. Heinzel, Nature 414 (2001) 345.
[4] K.D. Kreuer, Annual Review of Materials Research 33 (2003) 333.
[5] M. Mogensen, N.M. Sammes, G.A. Tompsett, Solid State Ionics 129 (2000) 63.
[6] H. Iwahara, T. Esaka, H. Uchida, N. Maeda, Solid State Ionics 3/4 (1981) 359.
[7] H. Iwahara, H. Uchida, K. Ono, K. Ogaki, Journal of the Electrochemical Society 135 (1988) 529.
[8] A.F. Sammells, R.L. Cook, J.H. White, J.J. Osborne, R.C. MacDuff, Solid State Ionics 52 (1992) 111.
[9] A.K. Demin, P.E. Tsiakaras, V.A. Sobyanin, S.Y. Hramova, Solid State Ionics 152–153 (2002) 555.
[10] T. Scherban, W.-K. Lee, A.S. Nowick, Solid State Ionics 28 (3) (1988) 585.
[11] N. Bonanos, B. Ellis, K.S. Knight, M.N. Mahmood, Solid State Ionics 35 (1989) 179.
[12] T. Higuchi, T. Tsukamoto, H. Matsumoto, T. Shimura, K. Yashiro, T. Kawada, J. Mizusaki, S. Shin, T. Hattori, Solid State Ionics 176 (2005) 2967.
[13] Q.L. Ma, R.R. Peng, Y.J. Lin, J.F. Gao, G.Y. Meng, Journal of Power Sources 161 (2006) 95.
[14] K. Xie, R. Yan, X. Chen, D. Dong, S. Wang, X. Liu, G. Meng, Journal of Alloys and Compounds 472 (2009) 551.
[15] K.D. Kreuer, Solid State Ionics 97 (1997) 1.
[16] T. Norby, Y. Larring, Current Opinion in Solid State & Materials Science 2 (1997) 593.
[17] Z. Tao, Z. Zhu, H. Wang, W. Liu, Journal of Power Sources 195 (2010) 3481.
[18] L. Bi, Z. Tao, W. Sun, S. Zhang, R. Peng, W. Liu, Journal of Power Sources 191 (2009) 428.
[19] W. Sun, L. Yan, Z. Shi, Z. Zhu, W. Liu, Journal of Power Sources 195 (2010) 4727.
[20] Y. Yamazaki, R. Hernandez-Sanchez, S.M. Haile, Chemistry of Materials 21 (2009) 2755.
[21] A. Magrasó, M.-L. Fontaine, Y. Larring, R. Bredesen, G.E. Syvertsen, H.L. Lei, T. Grande, M. Huse, R. Strandbakke, R. Haugsrud, T. Norby, Fuel Cells (2010), doi:10.1002/fuce.201000052.
[22] T. Omata, K. Okuda, S. Tsugi moto, S. Otsuka-Matsuo-Yao, Solid State Ionics 104 (1997) 249.
[23] J.-D. Wang, Y.-H. Xie, Z.-F. Zhang, R.-Q. Liu, Z.-J. Li, Materials Research Bulletin 40 (2005) 1294.
[24] S. Fang, L. Bi, L. Yan, W. Sun, C. Chen, W. Liu, Journal of Physical Chemistry C 114 (2010) 10986.
[25] L. Bi, S.Q. Zhang, S.M. Fang, L. Zhang, K. Xie, C.R. Xia, W. Liu, Electrochemistry Communications 10 (2008) 1005.
[26] L. Bi, S. Zhang, L. Zhang, Z. Tao, H. Wang, W. Liu, International Journal of Hydrogen Energy 34 (2009) 2421.
[27] R.R. Peng, Y. Wu, L.Z. Yang, Z.Q. Mao, Solid State Ionics 177 (2006) 389.
[28] L. Zhang, S.P. Jiang, W. Wang, Y.J. Zhang, Journal of Power Sources 170 (2007) 55.
[29] X. Zhang, M. Robertson, C. Decès-Petit, W. Qu, O. Kesler, R. Maric, d. Ghosh, Journal of Power Sources 175 (2008) 800.
[30] D. Yang, X. Zhang, C. Decès-Petit, R. Hui, R. Maric, d. Ghosh, Journal of Power Sources 164 (2006) 182.